

## Substituted Thiols in Dynamic Thiol–Thioester Reactions

Nicholas J. Bongiardina, Katelyn F. Long, Maciej Podgórski, and Christopher N. Bowman\*

Cite This: *Macromolecules* 2021, 54, 8341–8351

Read Online

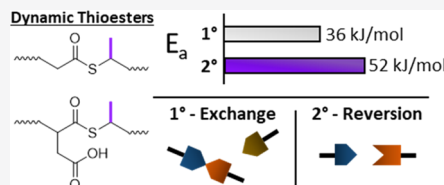
ACCESS |

Metrics &amp; More

Article Recommendations

Supporting Information

**ABSTRACT:** The thiol–thioester reaction has emerged as a promising method for developing covalent adaptable networks (CANs) due to its ability to exchange rapidly under low temperature conditions in a number of solvents, orthogonality among other functional groups, and tunability. Here, the effects of thiol substitution (i.e., primary vs secondary) were assessed with respect to their reactivity in two dynamic thioester reactions: the thiol–thioester exchange and the reversible thiol–anhydride addition. Model NMR experiments were conducted using small-molecule compounds to observe how polymers of similar components would behave in thiol–thioester exchange. It was determined that the  $K_{eq}$  was near unity for mixtures of primary thiols and secondary thioesters, and vice versa, in both a polar solvent,  $DMSO-d_6$ , and at most slightly favors primary thioesters in a relatively nonpolar solvent,  $CDCl_3$ . Dielectric spectroscopy and stress relaxation experiments were used to determine the relaxation times and activation energies of the two thioester-containing networks: Thiol-ene networks, which undergo thioester exchange, displayed activation energies of 73 and 71 kJ/mol from dielectric measurements and 36 and 53 kJ/mol from stress relaxation for the primary and secondary thiols, respectively. Thiol–anhydride-ene networks, which undergo both thioester exchange and reversible thiol–anhydride addition, displayed activation energies of 94 and 114 kJ/mol from dielectric and 111 and 139 kJ/mol from stress relaxation for primary and secondary thiols, respectively. In both types of networks, the secondary thioester-based networks demonstrated slower dynamics as compared to the same primary network by at least one order of magnitude. In the anhydride network, the secondary thiol also biased the dynamics toward reversible addition.

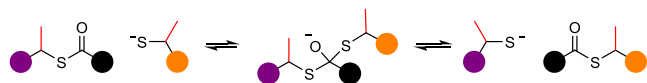


### INTRODUCTION

Covalent adaptable networks (CANs) are a class of thermosetting polymer materials that contain dynamic chemical functionalities that enable the rearrangement of what would normally be considered a static network. This dynamic character combines the mechanical robustness and chemical stability of thermosets with the processability and recyclability of thermoplastics. As such, these hybrid materials enable a unique array of material characteristics that are typically unattainable for thermosets, opening potential applications for which neither conventional thermoplastics nor thermosets are well suited.

The basic principle for producing CANs involves the incorporation of labile chemical bonds that are triggered by application of an external stimulus, such as light or heat. Depending on the choice of chemistry, the dynamic bonds either (i) break and reform via reversible addition or a dissociative mechanism, as is the case for the Diels–Alder reaction,<sup>1,2</sup> or (ii) may interconvert via a reversible exchange or an associative mechanism, as observed for transesterification,<sup>3</sup> disulfide exchange,<sup>4</sup> and thiol–thioester exchange.<sup>5,6</sup> In particular, thiol–thioester exchange (TTE) (Scheme 1) has received increased attention because of its low activation energy threshold (~30 kJ/mol), exchange rates that are tailored by the choice and concentration of a basic or nucleophilic catalyst, and the facile incorporation of thioesters into thiol–X-based materials.<sup>5–8</sup> This exchange moiety has shown great potential for peptide synthesis,<sup>9,10</sup> dissolvable

**Scheme 1. General Scheme for the Thiol–Thioester Exchange Reaction for Both Primary and Secondary (Red Line) Thiols/Thioesters**

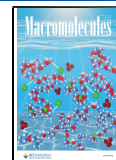


sealants,<sup>11</sup> pressure-sensitive adhesives,<sup>12</sup> and nanocomposites.<sup>12,13</sup>

While substantial work has been done to characterize TTE for thiols common in materials synthesis,<sup>5</sup> the effect of substitution of the thiol on TTE has received little attention. Recently, the substitution of the thiol on various thiol–X processes has seen attention from Li and co-workers, who observed that increasingly substituted thiols have a longer shelf life and less odor than typical primary thiols,<sup>14</sup> and Long and co-workers, who have shown that secondary and tertiary thiols can be used in thiol-ene<sup>15</sup> and thiol–Michael addition<sup>16</sup> polymerizations with minimal detrimental effects on reaction kinetics or conversion at relevant polymerization conditions

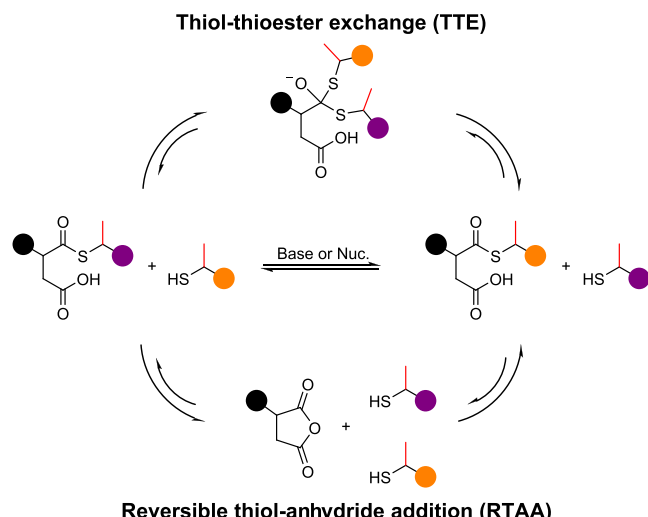
Received: March 24, 2021

Published: September 8, 2021



while resulting in the improved shelf life of the resin mixture. This outcome has important implications for many thiol–X materials that often cannot be premixed and stored as a monomer resin due to their high reactivity. As such, it is also useful to understand the effects of thiol substitution on TTE to further broaden the utility of this potent dynamic chemistry. Expanding upon classic thiol–ene systems for thioester chemistries, Podgórski and co-workers investigated dynamic thioester networks in which the thioester bonds were generated *in situ* in ring-opening thiol–anhydride additions.<sup>8,17</sup> These dynamic networks were composed of thioester bonds adjacent to the carboxylic acids, formed by a ring opening of the anhydride, and thioether bonds formed by the thiol–ene reaction. Importantly, these thioesters react both through a dissociative reaction, through reversible thiol–anhydride addition (RTAA), and an associative reaction, through TTE, depending on the amount of excess thiol, catalyst choice and concentration, and temperature (Scheme 2).

**Scheme 2.** General Scheme for Bond Rearrangement in Thiol–Anhydride-ene Materials<sup>a</sup>



<sup>a</sup>Shown on top is thiol–thioester exchange and shown on bottom is reversible thiol–anhydride addition. For simplicity, both reactions are generalized by showing thiols as the exchanging species.

In this work, experiments were performed to assess the advantages or disadvantages of using secondary thiols in thioester-based dynamic materials, both from a mechanistic standpoint and mechanical standpoint. Small model compounds, which are analogous to the monomers used in subsequent polymer studies, were synthesized, and thermodynamic equilibrium-driven reactions, similar to those described by Worrell and co-workers<sup>5</sup> using  $H^1$  NMR, were conducted to determine the relative reactivity and propensity for exchange of the primary and secondary thiols of interest. The impact of the substituted thioesters was then evaluated in two different thioester-containing networks: (1) thiol–ene networks similar to those studied by Worrell and co-workers<sup>5</sup> and (2) thiol–anhydride-ene networks as introduced by Podgórski and co-workers.<sup>8</sup> The differences in the dynamic character of the primary and secondary TE-containing networks were then evaluated using dielectric analysis (DEA) and compared to

conventional mechanical measurements from dynamic mechanical analysis (DMA).

## EXPERIMENTAL SECTION

**Materials.** Pentaerythritol tetrakis(3-mercaptopropionate) (PETMP), methyl 3-mercaptopropionate (MMP), 1,4-diazabicyclo[2.2.2]octane (DABCO), 4-(dimethylamino)pyridine (DMAP), allyl succinic anhydride (ASA), quinuclidine (QN), 1,3,5-trimethoxybenzene (TMB), triethylamine (TEA), the phosphine oxide photoinitiator Omnicure 819, 2,2-dimethoxy-2-phenylacetophenone (DMPA), and 1,1,3,3-tetramethylguanidine (TMG) were purchased from common stock chemical suppliers (Sigma-Aldrich, Fisher Scientific, TCI Chemicals) and used as delivered. Pentaerythritol tetrakis(3-mercaptopropionate) (PETMB) was generously provided by Showa Denko and used as delivered. Primary and secondary thioester-diene (1TE-diene and 2TE-diene, respectively) and methyl 3-mercaptopropionate (MMB) were synthesized as described in Appendix 1.

**Methods.**  $H^1$  NMR spectra were recorded in  $CDCl_3$  (internal standard: 7.26 ppm) and in  $DMSO-d_6$  (internal standard: 2.50 ppm, 1H) on a Bruker DRX-400 MHz spectrometer. See Appendix 2 for calibration curve preparation and experimental details. Chemical shifts ( $\delta$ ), reported in parts per million (ppm), had the following abbreviations used to identify the multiplicities: s, singlet; d, doublet; t, triplet; q, quartet; m, multiplet; b, broad.

**Sample Preparation for Thiol-ene Samples.** The monomer resin composed of a tetrathiol (1.0 equiv of PETMP or PETMB monomer), a thioester containing diene (1.0 equiv of either 1TE-diene or 2TE-diene monomer), 1 wt % Omnicure 819 (a phosphine oxide photoinitiator), and 4 mol % DABCO in TTE-active samples was prepared by first dissolving the photoinitiator and catalyst in the appropriate TE-diene and then mixing in the thiol. Dielectric samples were prepared on Mini-Varicon sensors purchased from Ambient Technologies. Sensors were rinsed with acetone and placed in a drying oven to remove adsorbed water and solvent from the surface. The cleaned sensor was placed flat on a glass slide and positioned under a curing light source with 250  $\mu$ m spacers on either side, and the monomer resin was deposited on the metal electrode surface and spread over the entire metal contact surface. A glass slide was placed on top and weighted down on each side with binder clips to avoid moving the layer up. The sample was irradiated with 405 nm at 25 mW/cm<sup>2</sup> for 5 min to activate the photoinitiator and cure the sample, which was then allowed to post-cure at 60 °C for 1 h. Samples for DMA and stress relaxation were prepared by depositing the resin between two glass slides with 250  $\mu$ m spacers, after which the sample was irradiated with 405 nm at 25 mW/cm<sup>2</sup> for 5 min, then post-cured at 60 °C for 1 hour.

**Sample Preparation of Thiol-ene-Anhydride Samples.** The procedure for sample preparation was adapted from a previously reported procedure.<sup>8</sup> The thiol monomer (1.0 equiv of PETMP or PETMB) and allyl succinic anhydride (2.0 equiv) were mixed. DMPA and DABCO were then dissolved in a small amount of DCM, then mixed with the monomer mixture, and allowed to rest for 0.5–1 h. DCM was then removed under vacuum, and the sample was subsequently cast and allowed to rest for 1 h to ensure maximum conversion of the anhydride moieties. Dielectric samples and DMA films were prepared with the same method described for the thiol-ene films. The thiol-ene reaction was then initiated by irradiation with 365 nm light at 25 mW/cm<sup>2</sup> for 5 min, then post-cured at 60 °C for 1 hour.

**Fourier Transform Infrared Spectroscopy (FTIR).** Thiol–anhydride-ene resins were prepared as described previously, and a drop of resin mixture was added between two clean salt plates before resting for 1 h and then cured as described above. The sample was then placed in a Nicolet 8700 and allowed to equilibrate at a given temperature from 40 to 120 °C. Once equilibrium was achieved as indicated by an unchanging FTIR spectrum, the time required to equilibrate was noted for dielectric analysis before the sample was heated to the next temperature.

**Dielectric Analysis (DEA).** Dielectric analysis was performed on a ModuLab XM Material Test System (AMETEK Scientific Instruments, UK) at various temperatures depending on the material. Isothermal temperature sweeps were performed over a range of  $30^{-2}$  to  $10^6$  Hz under an applied sinusoidal voltage of 4500 mV in amplitude. Samples were prepared on Mini-Varicon sensors as described above. Thiol-ene samples were allowed to equilibrate at a given temperature for 10 min before a spectrum was taken. Thiol-anhydride-ene samples were allowed to equilibrate for the time needed to reach a stable anhydride concentration as determined by FTIR, as described above.

**Dynamic Mechanical Analysis and Stress Relaxation.** Glass transition temperature ( $T_g$ ), storage modulus ( $E'$ ), and loss modulus ( $E''$ ) were measured on an RSA G2 dynamic mechanical analyzer (TA Instruments) using a temperature ramp rate of  $3\text{ }^{\circ}\text{C}/\text{min}$  and a frequency of 1 Hz with an oscillating strain of 0.03% and a preload force of 0.40 N. Stress relaxation was performed in tension. A strain of 8% was applied, and the resulting isothermal stress was measured over time at various temperatures and then normalized to the initial value.

## RESULTS AND DISCUSSION

**Model Compound Studies.** In their work on thioester exchange reaction in organic media, Worrell and co-workers<sup>5</sup> investigated the equilibrium constants for a variety of thiols and thioesters in a range of solvents to determine (i) the favored products at equilibrium for different thiol/thioester structures and (ii) which solvents were conducive to the exchange reaction. Their approach was adopted here to determine whether primary or secondary thiol/thioester products are favored when a primary thiol reacts with a secondary thioester and vice versa. The primary and secondary thiols and thioesters used in this study are shown in Figure 1a,

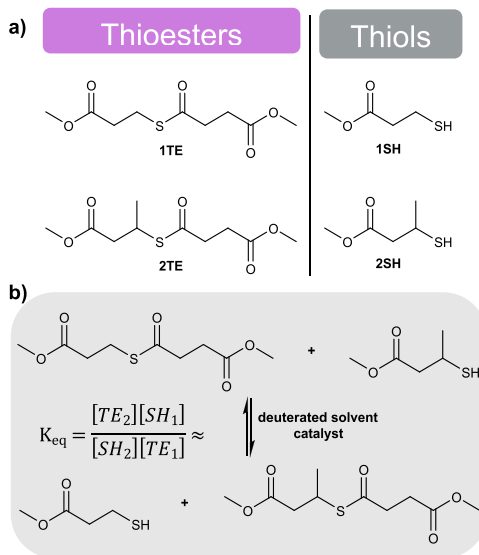


**Figure 1.** (a) Model primary and secondary thiol and thioester compounds used in NMR studies and (b) reaction scheme for exchange of primary and secondary model compounds and the definition of  $K_{eq}$  where the reactants and products can be either primary thiol and secondary thioester or vice versa.

and the reaction scheme used to calculate the equilibrium constant,  $K_{eq}$ , for each mixture as well as the definition of  $K_{eq}$  is provided in Figure 1b. Here, the  $K_{eq}$  for every mixture was calculated with the primary thioester and the secondary thiol as the reactants and the secondary thioester and primary thiol as the products. This approach was used to simplify the

comparison of the equilibrium constants, regardless of which thiol/thioester pair was used as the starting material. The investigation was carried out with the basic catalyst TMG ( $pK_a = 13.6$  in water), with the nucleophilic catalyst QN ( $N = 20.5$ ), or without any catalyst. These catalysts were selected because of their potent catalytic activity as determined in previous studies on TTE reactions relative to other catalysts. Tests were performed directly in deuterated solvents,  $\text{DMSO}-d_6$  or  $\text{CDCl}_3$ , to examine the effect of solvent polarity on equilibrium. The designations “a” and “b” denote whether the initial mixture contained a primary thiol and secondary thioester or a secondary thiol and primary thioester, respectively. Calibration curves were prepared for each thiol and thioester model compound (see Appendix 2, Supporting Information, for details) to compare the experimental thioester concentrations to an internal standard to correct for instrumental error and any solvent evaporation. Exchange reactions proceeded at room temperature until the reactions reached equilibrium—as indicated by two time points with a  $K_{eq}$  difference of  $<0.05$ —but all reactions were stopped after 150 h, and a reaction quotient ( $Q$ ) value was recorded if equilibrium had not yet been achieved, as occurred, for example, in the absence of any catalyst. Plots of the thioester content over time are provided in Figures S2–S6.

Shown in Table 1 are the equilibrium constants in  $\text{DMSO}-d_6$ , the more polar of the two solvents tested. The solutions with TMG as the catalyst (2a and 2b) achieved  $K_{eq}$ ’s of  $1.2 \pm 0.2$  and  $0.9 \pm 0.1$ , respectively. The quinuclidine solutions (3a and 3b) achieved  $K_{eq}$ ’s of  $0.9 \pm 0.2$  and  $0.82 \pm 0.08$ , respectively. These equilibrium constants are approximately unity, suggesting that neither the primary or secondary thiol nor thioester is significantly favored at equilibrium. Exchange also proceeded when no catalyst was present (1a and 1b) and did not reach full conversion after 150 h, reaching reaction quotients ( $Q$ ) of  $0.6 \pm 0.2$  and  $1.2 \pm 0.1$  in  $\text{DMSO}-d_6$  after 150 h while continuing to react slowly toward equilibrium.

Equilibrium constants in the less polar solvent,  $\text{CDCl}_3$ , are shown in Table 2. The TMG-containing solutions (4a and 4b) achieved  $K_{eq}$ ’s of  $0.61 \pm 0.1$  and  $0.5 \pm 0.1$ , respectively. The reactions with quinuclidine (5a and 5b) were incomplete after 150 h, reaching  $Q$ ’s of  $0.8 \pm 0.1$  and  $0.65 \pm 0.1$ , respectively. The equilibrium constants for the reaction catalyzed by TMG are again similar but slightly favoring the primary thioester. The quinuclidine-catalyzed reactions did not reach equilibrium because solvents of lower polarity are less conducive to rapid thiol–thioester exchange. This behavior is likely due to the sterically hindered nucleophilic mechanism for which the bulky zwitterionic intermediate will not be as well stabilized as in a more polar solvent. Since the TMG-catalyzed reaction went to completion and slightly favored the primary, steric hindrance plays an important role in nonpolar environments where thioester exchange tends to be less favorable. Because the exchange rate was significantly reduced in chloroform with a catalyst, noncatalyzed exchange reactions were not performed. Even though the base and nucleophile mechanisms differ slightly, it should be noted that the  $K_{eq}$  and  $Q$  values are comparable, as expected in the context of catalysis, regardless of whether a nucleophile (quinuclidine) or base (TMG) catalyst was used and are comparable to those reported in the literature.<sup>5</sup> In addition, longer times were required to reach equilibrium in  $\text{CDCl}_3$  compared to  $\text{DMSO}-d_6$ , not reaching equilibrium in the case of the quinuclidine-catalyzed solution.

Table 1. Summary of  $K_{eq}$  Values for All Solutions Studied<sup>a</sup>

solution	reactant	product	catalyst	$K_{eq}$ ( $Q^*$ )
1a	1° thioester + 2° thiol	2° thioester + 1° thiol	none	$0.61^* \pm 0.1$
1b	2° thioester + 1° thiol	1° thioester + 2° thiol	none	$1.2^* \pm 0.1$
2a	1° thioester + 2° thiol	2° thioester + 1° thiol	TMG	$1.2 \pm 0.2$
2b	2° thioester + 1° thiol	1° thioester + 2° thiol	TMG	$0.9 \pm 0.1$
3a	1° thioester + 2° thiol	2° thioester + 1° thiol	quinuclidine	$0.9 \pm 0.2$
3b	2° thioester + 1° thiol	1° thioester + 2° thiol	quinuclidine	$0.82 \pm 0.08$

<sup>a</sup>Values marked by an asterisk are reaction quotients because equilibrium was not reached by the end of experiment. Experiments were conducted in DMSO-*d*<sub>6</sub> at room temperature with 10 mol % catalyst. All reactions used equimolar thiol and thioester reactants and were compared to an internal standard (1,3,5-trimethoxybenzene). Time points were taken for up to 150 h or the achievement of equilibrium as indicated by a lack of further changes in the species concentrations. An asterisk (\*) represents an incomplete reaction, with the reaction quotient ( $Q$ ) given.

Table 2. Summary of  $K_{eq}$  Values for CDCl<sub>3</sub> Solutions<sup>a</sup>

solution	reactant	product	catalyst	$K_{eq}$ ( $Q$ )
4a	1° thioester + 2° thiol	2° thioester + 1° thiol	TMG	$0.61 \pm 0.1$
4b	2° thioester + 1° thiol	1° thioester + 2° thiol	TMG	$0.5 \pm 0.1$
5a	1° thioester + 2° thiol	2° thioester + 1° thiol	quinuclidine	$0.8^* \pm 0.1$
5b	2° thioester + 1° thiol	1° thioester + 2° thiol	quinuclidine	$0.65^* \pm 0.1$

<sup>a</sup>Values marked by an asterisk are reaction quotients because equilibrium was not reached by the end of experiment. These experiments were conducted in CDCl<sub>3</sub> at room temperature with 10 mol % catalyst. All reactions used equimolar thiol and thioester reactants and were compared to an internal standard (1,3,5-trimethoxybenzene). Time points were taken for up to 150 h. An asterisk (\*) represents an incomplete reaction, with the reaction quotient ( $Q$ ) given.

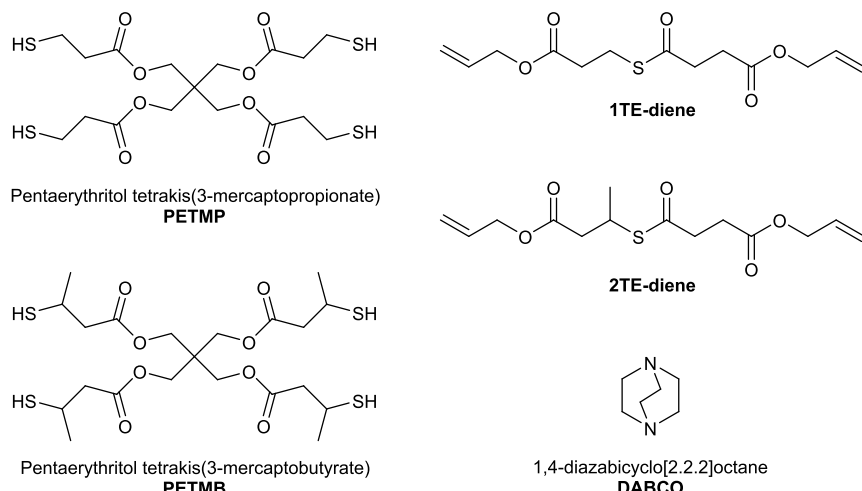


Figure 2. Structures of the thiols, thioesters, and nucleophilic catalyst for thiol-ene films. Samples consisted of a 2:1 ratio of thiol-to-thioester functionality with 1 wt % of the visible light photoinitiator I819 and were irradiated at 25 mW/cm<sup>2</sup>.

This delay was expected given that thioester exchange does not occur as efficiently in nonpolar media such as CDCl<sub>3</sub>.

**Thiol-ene Materials.** An important feature of any CAN is the rate of exchange when the chemistry is active. While NMR studies of model compounds show that an equilibrium mixture of primary thioester and secondary thiol or vice versa does not strongly favor one product, equilibrium on its own does not provide information about the exchange rates. To this end, thiol-ene networks based on the previous literature<sup>5,6</sup> with either primary or secondary thiols/thioesters were made as shown in Figure 2. Here, DABCO was selected as a nucleophilic catalyst because of its good nucleophilicity and solubility in the monomer resins and ability to remain stable over longer periods of time compared to quinuclidine. Different from what was observed for structurally similar thiol-ene and thiol-Michael networks,<sup>15,16</sup> the glass transition temperatures for the secondary thiol-containing networks were

slightly higher ( $-20$  °C vs  $-25$  °C without DABCO for the primary thiol and  $-13$  °C vs  $-14$  °C without a catalyst for the secondary thiol) (Figure S7), while the catalyst had little effect on the  $T_g$ . Dielectric and mechanical stress relaxation measurements were used to assess the relative effectiveness and rates of TTE for these primary thioester- and secondary thioester-based materials. It is hypothesized that due to the steric hindrance of the secondary thioester and thiol monomers, the overall dynamics are slower than for the primary system despite the comparative thermodynamic equilibria as assessed in model systems.

**Dielectric Analysis of Thiol-ene Networks.** Dielectric analysis (DEA) is an important tool in polymer dynamic research due to its unique capability to efficiently probe different chain relaxation modes over wide temperature and frequency ranges. An oscillating electric field is applied and interacts with the permanent and induced dipole moments in

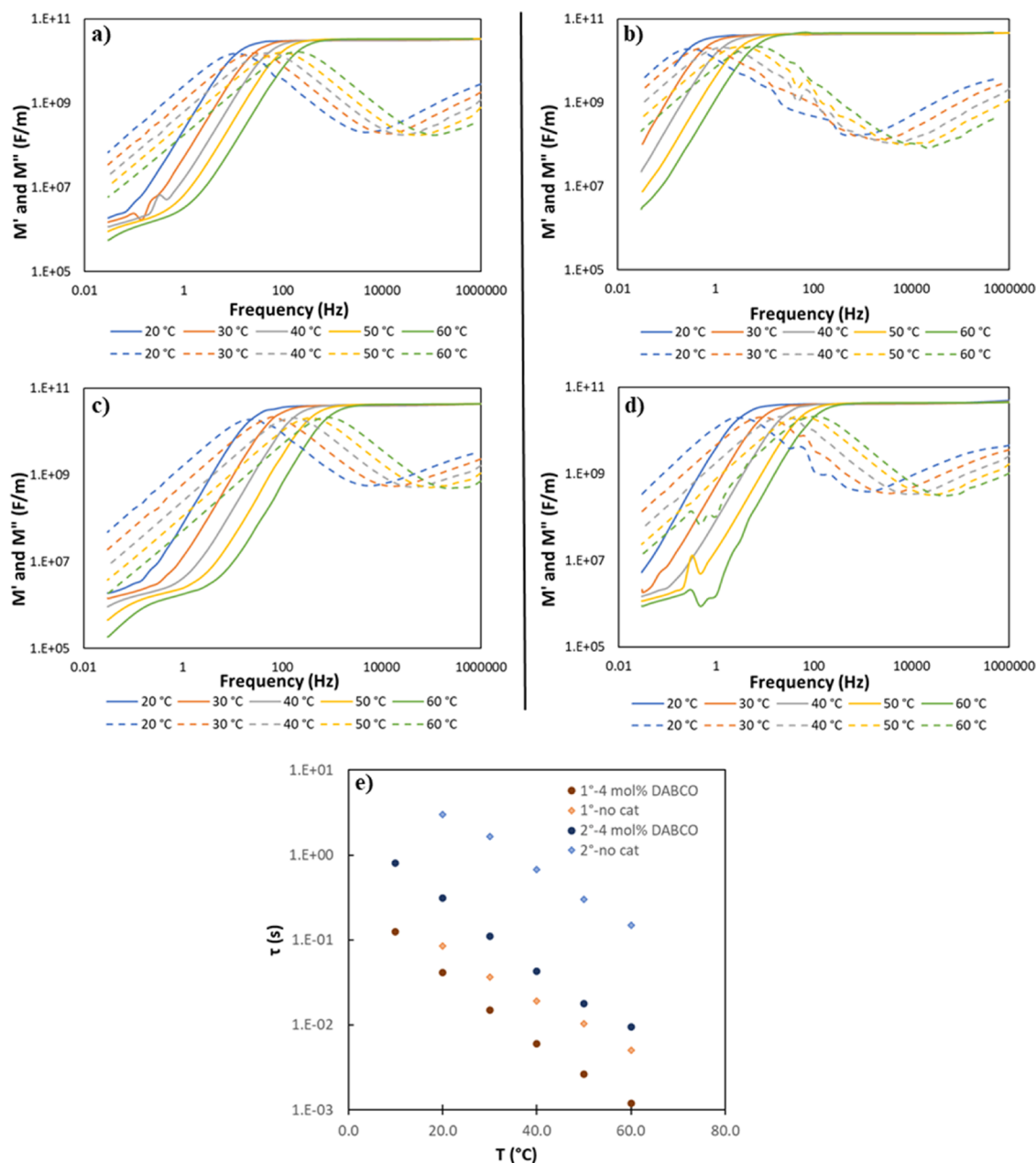


**Figure 3.** Representative dielectric spectra for thioester films taken using an interdigital sensor at various temperatures: primary thiol/thioester sample containing (a) no catalyst and (c) 4 mol % DABCO as a nucleophilic catalyst and secondary thiol/thioester sample containing (b) no catalyst and (d) 4 mol % DABCO as a nucleophilic catalyst. The solid lines denote the real electric modulus, and the dashed lines denote the loss electric modulus. (e) Relaxation times as a function of temperature for the primary and secondary thioester films, both with and without a catalyst.

the polymer. The response and relaxation of these dipoles can then be leveraged to probe the structure and properties of the material of interest. The ability to use an oscillating electric field over a larger frequency range than mechanical analyses such as DMA (up to  $10^6$  Hz for DEA compared to  $10^2$  Hz in DMA) enables one to observe dynamics at the chain and chain-segment scale in a way that is impractical or impossible by macroscopic mechanical testing, provided that the material of interest possesses polar groups to interact with this electric field. A variety of polymer systems have been assessed using DEA, including epoxy resin systems that are ubiquitous in materials applications,<sup>18</sup> natural and synthetic rubbers,<sup>19,20</sup> dental resins,<sup>21</sup> and composites to probe filler/resin/interface dynamics.<sup>22–24</sup> However, despite its appropriateness for

probing molecular dynamics, there has been little work to use DEA to evaluate polymer dynamics in CANs. Moreover, DEA offers a direct approach to explore how introducing a simple structural modification, in this case, the methyl groups associated with thiol/thioester substitution, affects the bond exchange and the overall dynamics of the network.

Here, DEA was used to assess the real ( $M'$ ) and loss ( $M''$ ) electric moduli with respect to the  $\alpha$ -relaxation, which is associated with segmental chain motions and the glass transition, for primary and secondary TTE networks. Figure 3 shows  $M'$  and  $M''$  for primary and secondary thio-ene networks that contain the nucleophilic catalyst DABCO (Figure 3a,b, respectively) and those that did not contain a catalyst (Figure 3c,d, respectively). Measurements were taken

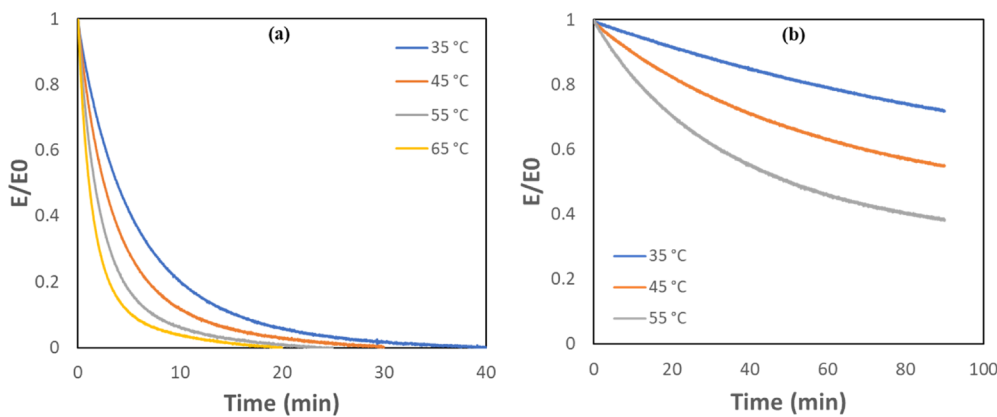


**Figure 4.** Representative stress relaxation data at various temperatures for (a) the primary thiol–thioester material and (b) the secondary thiol–thioester material.

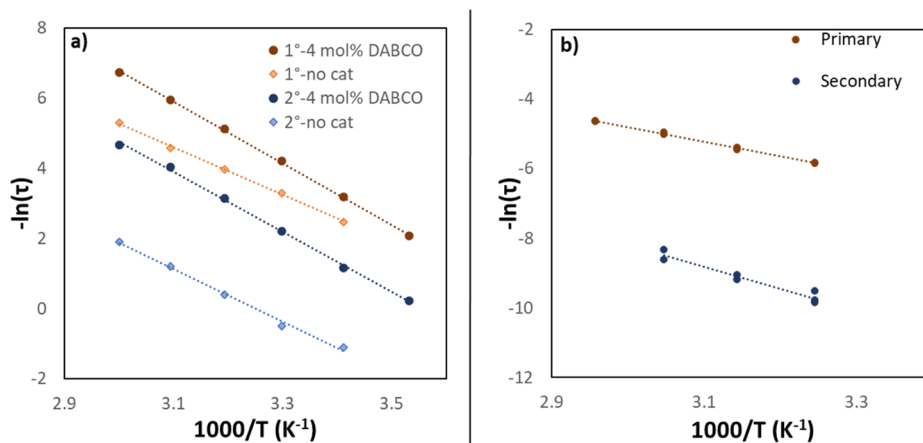


**Figure 5.** Arrhenius plots of (a) the  $\alpha$ -relaxation times from dielectric measurements for the primary and secondary thiol-ene samples, both with (diamonds) and without (circles) 4 mol % DABCO as a nucleophilic catalyst, and (b) the relaxation times measured by stress relaxation with 4 mol % DABCO. Dashed lines indicate a linear fit to the data.

over a frequency range of  $30^{-2}$  to  $10^6$  Hz for a temperature range of 20–60 °C. The frequency of the maximum of  $M''$  was taken to determine the relaxation time at a given temperature and was determined by a Cole–Cole fit of the modulus curves (Appendix 3, Supporting Information). This fit was used to accurately determine the frequency that corresponds to the peak; these relaxation times as a function of temperature are shown in Figure 3e.

For both the primary and secondary thioester networks, the  $\alpha$ -relaxation time is faster when 4 mol % DABCO is present compared to the uncatalyzed network over the entire temperature range. The primary relaxation rate increases by a factor of 2 to 4, while the rate for the secondary networks increases by an order of magnitude. These faster dynamics for both primary and secondary networks arise from increased mobility via network rearrangement enabled by TTE when a catalyst is present. Now, comparing the primary and secondary thioester networks' relaxation times with 4 mol % DABCO, the primary network shows faster dynamics at every temperature, roughly by a factor of 7. This behavior indicates that TTE is faster for primary thiols/thioesters, where steric hindrance due to the methyl substitution in the secondary thioester is likely a major contributor to slower dynamic bond rearrangement.

At the same time, when a catalyst is not present, the relaxation times for the primary thioester are substantially faster in this dielectric measurement, by roughly a factor of 35,

as compared to the equivalent secondary network, even though little dynamic covalent behavior occurs without a catalyst (Figure S8). A possible explanation for this behavior is that the large number of methyl groups in the secondary thiols and thioesters increases steric hindrance while reducing the overall polarity of the network, which is known to decrease the rate of TTE because more polar media are conducive to the movement of charged/polar species through the material.<sup>5</sup> This decrease in polarity may therefore lead to a decrease in mobility, resulting in a slower relaxation time when no catalyst is present in otherwise equivalent networks. Therefore, polarity will also affect the catalyzed networks in addition to any steric effects that arise from substitution of the thiols and thioesters.

**Stress Relaxation of Thiol-ene Networks.** To validate DEA measurements, stress relaxation experiments were performed at constant temperatures and strain in tension (8%) to mechanically determine relaxation times due to TTE, as shown in Figure 4. The relaxation rate is significantly slower in the secondary thiol-based material. For example, the mechanical relaxation times at 35 °C for the primary network relaxation times are nearly two orders of magnitude faster (~5.5 min) at the same catalyst concentration as compared to the secondary thioester-based network (~315 min). Confirming the dynamics measured by DEA, this behavior indicates that the secondary network exhibits slower covalent bond rearrangement as compared to the primary thioester network.

Stress relaxation in control networks without a catalyst was also evaluated at 35 and 65 °C, and only a small amount of relaxation was observed at 65 °C for the primary thioester (~5% relaxation) and none for the secondary thioester (Figure S8). Slower relaxation times for the secondary thioester network are attributed to a combination of steric hindrance and a decrease in polarity associated with the methyl groups.

The relaxation times from both DEA and stress relaxations were used to calculate the activation energies, all measured within the temperature range from 35 to 65 °C. Arrhenius plots of relaxation times from DEA and stress relaxation are shown in Figure 5a,b. As discussed for the dielectric measurements, the primary thiol/thioester materials exhibit fast relaxation times at all temperatures compared to their secondary counterparts, regardless of whether DABCO was included. Mechanical stress relaxation times follow the same trend. The activation energies extracted from a linear regression of the Arrhenius plots are provided in Table 3.

**Table 3. Activation Energies as Calculated from Arrhenius Fits of the Dielectric Loss Peaks and Stress Relaxation Times<sup>a</sup>**

	<i>E<sub>a</sub></i> (kJ/mol)	
	primary	secondary
control (DEA)	56 ± 1	63 ± 3
4% DABCO (DEA)	72.9 ± 0.8	71 ± 1
4% DABCO (SR)	36.1 ± 0.6	52 ± 6

<sup>a</sup>Errors indicated are the standard error of the regression.

The activation energies extracted from DEA for the networks containing DABCO are indistinguishable for the primary and secondary networks (73 and 71 kJ/mol, respectively) despite the slower rate at which relaxation occurs

in the secondary networks. These energies differ from those extracted from the mechanical relaxation times, which were 36 and 52 kJ/mol, respectively. The discrepancy between these two measurements is likely due to inherent differences in the size scales and types of molecular motions probed by dynamic dielectric spectroscopy versus mechanical stress relaxation methodologies.<sup>25</sup> For example, in simultaneous DEA–DMA measurements of a curing network, DMA is able to measure the gelation point resulting from a rapid increase in the storage modulus, while DEA can measure the decrease in chain mobility after gelation that does not show up in mechanical moduli.<sup>26</sup>

At the same time, control materials without a catalyst show a slightly higher activation energy for the secondary network (63 vs 56 kJ/mol), although the difference is relatively small. Any difference is likely due to decreased polarity of the secondary network, as discussed previously. Further, the catalyzed networks did not show the same difference in activation energy because of the increased polarity and mobility introduced by additional charged species during exchange, which is a result of the reaction of the nucleophile with thioester carbonyl groups that participate in dynamic exchange.

**Thiol–Anhydride–ene Network.** Another CAN system of interest that leverages thioesters is the thiol–anhydride–based network as introduced by Podgórski and co-workers.<sup>8</sup> The monomers and reaction scheme are shown in Figure 6a,b, respectively. In a thiol–anhydride dynamic network, an interesting feature is introduced to the TTE paradigm because the formed thioesters are adjacent to a carboxylic acid product upon ring opening of the anhydride by a thiol. Because this neighboring carboxylic acid is six atoms away from the sulfur in the thioester, this adduct has been shown to undergo both dynamic ring-closing/opening (dissociation) reactions as well as the TTE (association) reaction as observed in the more conventional thiol–ene materials shown previously, depending

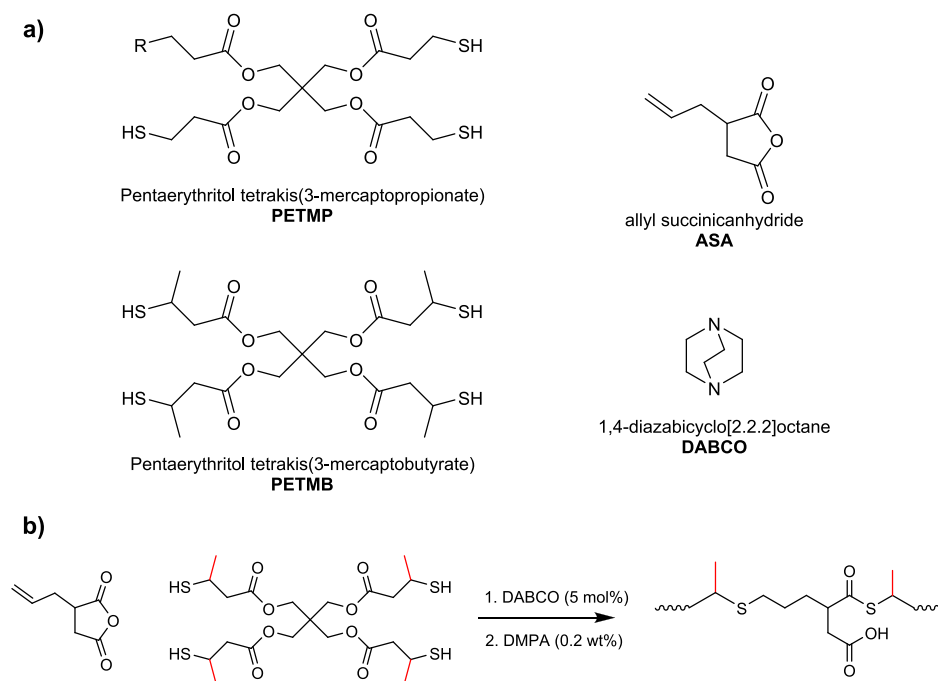


**Figure 6.** (a) Structures of the thiols, anhydride, and nucleophilic catalyst for thiol–anhydride–ene films. Samples consisted of a 2:1 ratio of thiol-to-thioester functionality with 0.2 wt % of the UV light photoinitiator DMPA and were irradiated at 25 mW/cm<sup>2</sup>. (b) General scheme for the thiol–anhydride–ene reaction.

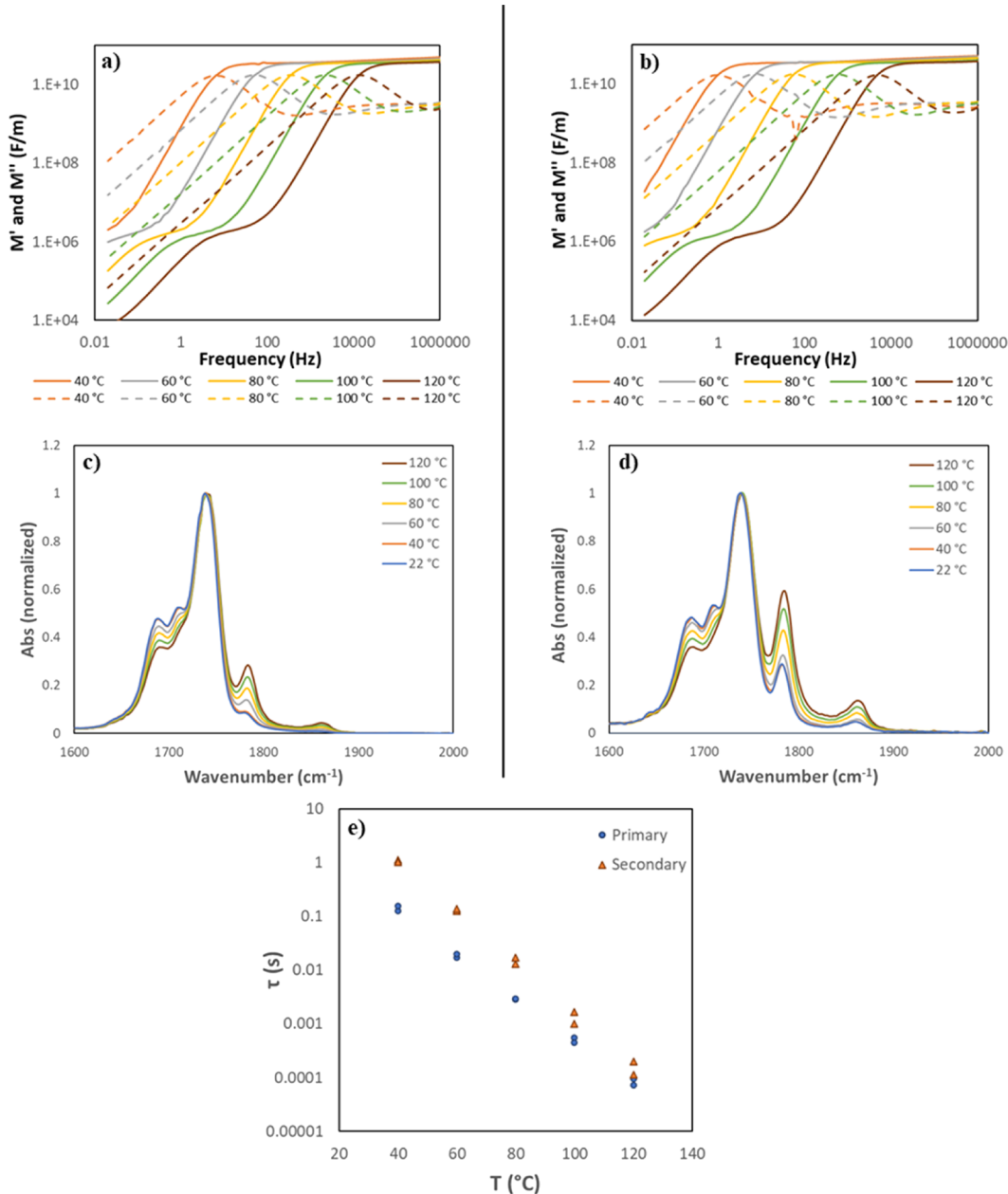


**Figure 7.** Representative dielectric spectra of (a) the primary and (b) secondary thiol-anhydride-ene samples at various temperatures. Dashed lines in the dielectric spectra represent the loss electric modulus ( $M''$ ), and solid lines represent the real electric modulus ( $M'$ ). The IR peak corresponding to the anhydride, highlighted in gray, appears at approximately  $1770\text{ cm}^{-1}$  and is shown for (c) primary and (d) secondary thiol-anhydride-ene networks at the same temperatures as the dielectric spectra as well as room temperature. (e) Relaxation time, as determined by a Cole-Cole fit, as a function of temperature for the dielectric spectra.

on the reaction temperature and the amount of excess thiol present in the network. Like the thiol-ene system discussed previously, it is expected that the secondary thiol-anhydride-ene network will show slower dynamics with respect to the TTE reaction, or associative character, compared to the primary material due to steric considerations. However, steric hindrance may also increase the prevalence of the ring-closing/opening reaction pathway, or dissociative character, in the secondary thiol-thioester-based material.

**Dielectric Analysis of Thiol-Anhydride-ene Networks.** Thiol-anhydride-ene materials enable tuning of the prevalence of reversible addition versus reversible exchange by changing the temperature, catalyst type, and/or catalyst concentration. Thiol substitution represents another tool through which these

relative rates are tuned. Both networks possess similar glass transition temperatures around  $11\text{ }^\circ\text{C}$  despite the secondary network having a lower rubbery storage modulus. (Figure S9). Figure 7a,b shows the dielectric spectra for primary and secondary thiol-anhydride-ene materials, respectively, and Figure 6e shows the relaxation times at each temperature for both networks. As seen in Figure 6e, a clear shift to slower relaxation times is seen for the secondary thiol-based material. However, the relaxation times for both primary and secondary thioesters converge at higher temperatures, narrowing from a difference of a factor of 7 at  $40\text{ }^\circ\text{C}$  to a factor of roughly 1.8 at  $120\text{ }^\circ\text{C}$ . Considering the slower TTE dynamics associated with secondary thiols (as observed for the thiol-ene networks discussed in the previous section), converging relaxation times

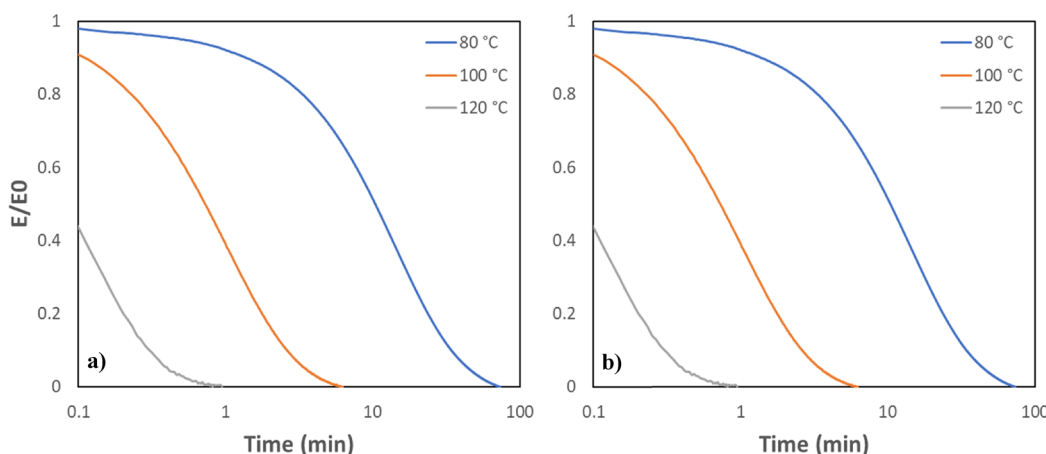


**Figure 8.** Representative stress relaxation data, given as the normalized modulus, at various temperatures for (a) the primary thiol–anhydride-ene and (b) secondary thiol–anhydride-ene materials.

suggests that the secondary thioester is reverting to the anhydride and thiol to a greater extent than the primary thioesters, which decreases cross-linking and, by extension, increases mobility and, therefore, the relaxation rate. Indeed, a greater extent of the ring-closing reaction is observed in the IR spectra taken at the same temperatures as the dielectric measurements, as shown in Figure 7c,d. These IR spectra are normalized to the carbonyl peak at  $1740\text{ cm}^{-1}$ , which corresponds to the ester present in both thiol monomers, which is not expected to change with temperature.

Here, a clear increase in anhydride content is seen at  $1770\text{ cm}^{-1}$  (highlighted in gray) for both the primary and secondary networks. However, the intensity of the anhydride peak is higher for the secondary thioester network at every temperature as compared to the primary network. This behavior indicates that the secondary network has a higher propensity to undergo reversion to the thiol and anhydride rather than TTE. This is most likely due to the increased steric hindrance of the secondary thiol, shifting the equilibrium toward the less sterically hindered anhydride/thiol products. As confirmation, a decrease in cross-linking at higher temperatures is also reflected by a drop-off in the rubbery storage modulus in DMA measurements (Figure S9) at about  $100\text{ }^\circ\text{C}$  for the secondary network as compared to the primary network at  $120\text{ }^\circ\text{C}$ .

**Stress Relaxation of Thiol–Anhydride-ene Materials.** Stress relaxation experiments were performed (5% strain) to complement the DEA measurements as provided in Figure 8a,b for the primary and secondary thioester materials, respectively. Both materials relax stress over this temperature range. The primary network relaxes faster at  $80\text{ }^\circ\text{C}$  with a relaxation time of 11 min compared to 13 min for the secondary network. However, as the temperature increases to  $120\text{ }^\circ\text{C}$ , the secondary network becomes more rapid with a relaxation time of 6 s compared to 14 s for the primary.

This behavior matches well with observations in DEA and IR, as discussed in Figure 7, that the secondary network has a higher propensity to undergo reversible addition at an increased temperature, resulting in fewer cross-links compared to the primary network at the same temperature and, therefore, faster relaxation. The ability to bias these thiol–anhydride-ene materials toward associative or dissociative rearrangement by simply increasing the substitution of the thiol is a facile tool for controlling dynamic behavior in a unique manner. Arrhenius plots for the relaxation times from DEA and stress relaxation

are provided in Figure S10a,b, respectively, and the activation energies determined by linear regression are provided in Table 4.

**Table 4. Activation Energies as Calculated from Arrhenius Fits of the Dielectric Loss Peaks and Stress Relaxation Times for the Thiol–Anhydride-ene Materials<sup>a</sup>**

	$E_a$ (kJ/mol)	
	primary	secondary
DEA	$94 \pm 2$	$114 \pm 4$
stress relaxation	$111 \pm 3$	$139 \pm 6$

<sup>a</sup>Errors indicated are the standard error of the regression.

The activation energy of the secondary thiol is higher in both the dielectric measurement,  $114\text{ kJ/mol}$  compared to  $94\text{ kJ/mol}$ , and stress relaxation,  $139\text{ kJ/mol}$  compared to  $111\text{ kJ/mol}$ , although the primary and secondary thiols differ more in stress relaxation than in DEA. A similar trend was observed for the thiol-ene networks, where DEA detected no significant difference in activation energy between the primary and secondary networks, but a substantial difference was measured by stress relaxation. Here, the fundamental difference is that unlike the thiol-ene networks, reversible addition also occurs in the thiol–anhydride-ene network. This changes the network structure as the temperature increases to a greater extent in the secondary network than in the primary network, and DEA is capable of detecting these changes in mobility when bonds form or, in this case, break.<sup>26</sup> Depolymerization due to reversible addition also changes the polarity in addition to the structure because the thioesters and their adjacent carboxylic acids convert back to thiols and anhydrides. This shift in polarity may very well translate into similar trends in the activation energy for both DEA and stress relaxation. Improving our understanding of how dynamic bonds impact dielectric behavior in CANs is a continued area of interest in future investigations.

## CONCLUSIONS

The substitution of the thiol in dynamic thioester reactions was shown to have a significant impact on material behavior. Model studies demonstrated that the primary thiol/thioester is not strongly favored over the secondary thiol/thioester at

equilibrium in thiol–thioester exchange in media that is conducive to thioester exchange, and exchange occurs even without a base or nucleophilic catalyst, albeit much more slowly. In addition, the exchange was significantly slowed in a low-polarity solvent. These same primary and secondary thioester functionalities in thiol–ene networks undergo dynamic exchange over the same temperature range, but the secondary thiol–thioester network showed a far slower exchange rate in both dielectric analysis and stress relaxation experiments due to decreases in polarity and increased steric hindrance associated with secondary thiols and thioesters. Finally, thiol–anhydride–ene networks, which enable both reversible addition and reversible thioester exchange, show that using a secondary thiol/thioester biases exchange toward reversible addition in a stoichiometric system due to the steric hindrance of the methyl substitution. In both networks, slower exchange kinetics in the secondary materials are attributed to increased steric hindrance and a decrease in polarity associated with the methyl substitution.

## ■ ASSOCIATED CONTENT

### Supporting Information

The Supporting Information is available free of charge at <https://pubs.acs.org/doi/10.1021/acs.macromol.1c00649>.

Experimental details, synthetic procedures, calibration curves and model study controls, dielectric fitting, and NMR spectra of synthesized molecules ([PDF](#))

## ■ AUTHOR INFORMATION

### Corresponding Author

Christopher N. Bowman – *Material Science and Engineering Program, University of Colorado, Boulder, Colorado 80309, United States; Department of Chemical and Biological Engineering, University of Colorado at Boulder, Boulder, Colorado 80309, United States; [ORCID.org/0000-0001-8458-7723](#); Email: [christopher.bowman@colorado.edu](mailto:christopher.bowman@colorado.edu)*

### Authors

Nicholas J. Bongiardina – *Material Science and Engineering Program, University of Colorado, Boulder, Colorado 80309, United States*

Katelyn F. Long – *Department of Chemistry, University of Colorado, Boulder, Colorado 80309, United States*

Maciej Podgórski – *Department of Polymer Chemistry, Institute of Chemical Sciences, Faculty of Chemistry, Maria Curie-Skłodowska University, Lublin 20-031, Poland; Department of Chemical and Biological Engineering, University of Colorado at Boulder, Boulder, Colorado 80309, United States*

Complete contact information is available at:

<https://pubs.acs.org/10.1021/acs.macromol.1c00649>

### Notes

The authors declare no competing financial interest.

## ■ ACKNOWLEDGMENTS

This work was supported by the U.S. National Institutes of Health (1 F31 DE027861-01A1 and 5 F31 DE027880-02) and the National Science Foundation (CHE 1808484).

## ■ REFERENCES

- (1) Zhang, G.; Zhao, Q.; Yang, L.; Zou, W.; Xi, X.; Xie, T. Exploring Dynamic Equilibrium of Diels–Alder Reaction for Solid State Plasticity in Remoldable Shape Memory Polymer Network. *ACS Macro Lett.* **2016**, *5*, 805–808.
- (2) Gandini, A. The furan/maleimide Diels–Alder reaction: A versatile click–unclick tool in macromolecular synthesis. *Prog. Polym. Sci.* **2013**, *38*, 1–29.
- (3) Capelot, M.; Montarnal, D.; Tournilhac, F.; Leibler, L. Metal-catalyzed transesterification for healing and assembling of thermosets. *J. Am. Chem. Soc.* **2012**, *134*, 7664–7667.
- (4) Lei, Z. Q.; Xiang, H. P.; Yuan, Y. J.; Rong, M. Z.; Zhang, M. Q. Room-Temperature Self-Healable and Remoldable Cross-linked Polymer Based on the Dynamic Exchange of Disulfide Bonds. *Chem. Mater.* **2014**, *26*, 2038–2046.
- (5) Worrell, B. T.; Mavila, S.; Wang, C.; Kontour, T. M.; Lim, C. H.; McBride, M. K.; Musgrave, C. B.; Shoemaker, R.; Bowman, C. N. A user's guide to the thiol–thioester exchange in organic media: scope, limitations, and applications in material science. *Polym. Chem.* **2018**, *9*, 4523–4534.
- (6) Worrell, B. T.; McBride, M. K.; Lyon, G. B.; Cox, L. M.; Wang, C.; Mavila, S.; Lim, C. H.; Coley, H. M.; Musgrave, C. B.; Ding, Y.; Bowman, C. N. Bistable and photoswitchable states of matter. *Nat. Commun.* **2018**, *9*, 2804.
- (7) Wang, C.; Mavila, S.; Worrell, B. T.; Xi, W.; Goldman, T. M.; Bowman, C. N. Productive Exchange of Thiols and Thioesters to Form Dynamic Polythioester-Based Polymers. *ACS Macro Lett.* **2018**, *7*, 1312–1316.
- (8) Podgórski, M.; Spurgin, N.; Mavila, S.; Bowman, C. N. Mixed mechanisms of bond exchange in covalent adaptable networks: monitoring the contribution of reversible exchange and reversible addition in thiol–succinic anhydride dynamic networks. *Polym. Chem.* **2020**, *11*, 5365–5376.
- (9) Dawson, P.; Muir, T.; Clark-Lewis, I.; Kent, S. Synthesis of proteins by native chemical ligation. *Science* **1994**, *266*, 776–779.
- (10) Konieczynska, M. D.; Villa-Camacho, J. C.; Ghobril, C.; Perez-Viloria, M.; Tevis, K. M.; Blessing, W. A.; Nazarian, A.; Rodriguez, E. K.; Grinstaff, M. W. On-Demand Dissolution of a Dendritic Hydrogel-based Dressing for Second-Degree Burn Wounds through Thiol–Thioester Exchange Reaction. *Angew. Chem. Int. Ed. Engl.* **2016**, *55*, 9984–9987.
- (11) Ghobril, C.; Charoen, K.; Rodriguez, E. K.; Nazarian, A.; Grinstaff, M. W. A dendritic thioester hydrogel based on thiol–thioester exchange as a dissolvable sealant system for wound closure. *Angew. Chem. Int. Ed. Engl.* **2013**, *52*, 14070–14074.
- (12) Dobson, A. L.; Bongiardina, N. J.; Bowman, C. N. Combined Dynamic Network and Filler Interface Approach for Improved Adhesion and Toughness in Pressure-Sensitive Adhesives. *ACS Applied Polymer Materials* **2020**, *2*, 1053–1060.
- (13) Sowan, N.; Lu, Y.; Kolb, K. J.; Cox, L. M.; Long, R.; Bowman, C. N. Enhancing the toughness of composites via dynamic thiol–thioester exchange (TTE) at the resin–filler interface. *Polym. Chem.* **2020**, *11*, 4760–4767.
- (14) Li, Q.; Zhou, H.; Hoyle, C. E. The effect of thiol and ene structures on thiol–ene networks: Photopolymerization, physical, mechanical and optical properties. *Polymer* **2009**, *8*, 2237.
- (15) Long, K. F.; Bongiardina, N. J.; Mayordomo, P.; Olin, M. J.; Oretiga, A. D.; Bowman, C. N. Effects of 1°, 2°, and 3° Thiols on Thiol–Ene Reactions: Polymerization Kinetics and Mechanical Behavior. *Macromolecules* **2020**, *53*, 5805–5815.
- (16) Long, K. F.; Wang, H.; Dimos, T. T.; Bowman, C. N. Effects of Thiol Substitution on the Kinetics and Efficiency of Thiol–Michael Reactions and Polymerizations. *Macromolecules* **2021**, *54*, 3093–3100.
- (17) Podgórski, M.; Mavila, S.; Huang, S.; Spurgin, N.; Sinha, J.; Bowman, C. N. Thiol–Anhydride Dynamic Reversible Networks. *Angewandte Chemie International Edition* **2020**, *59*, 9345–9349.
- (18) Jilani, W.; Mzabi, N.; Gallot-Lavallée, O.; Fourati, N.; Zerrouki, C.; Zerrouki, R.; Guermazi, H. Dielectric relaxations investigation of a

synthesized epoxy resin polymer. *The European Physics Journal Plus* **2015**, *130*, 76.

(19) Carrertero-Gonzalez, J.; Ezquerro, T. A.; Amnuaypornsri, S.; Toki, S.; Verdejo, R.; Sanz, A.; Sakdapipanich, J.; Hsiao, B. S.; López-Manchado, M. A. Molecular dynamics of natural rubber as revealed by dielectric spectroscopy: The role of natural cross-linking. *Soft Matter* **2010**, *6*, 3636–3642.

(20) Hernández, M.; Grande, A. M.; van der Zwaag, S.; García, S. J. Monitoring Network and Interfacial Healing Processes by Broadband Dielectric Spectroscopy: A Case Study on Natural Rubber. *ACS Appl. Mater. Interfaces* **2016**, *8*, 10647–10656.

(21) Lovell, L. G.; Berchtold, K.; Elliot, J. E.; Lu, H.; Bowman, C. N. Understanding the kinetics and network formation of dimethacrylate dental resins. *Polym. Adv. Technol.* **2001**, *12*, 335–345.

(22) Tsangaris, G. M.; Psarras, G. C.; Kouloumbi, N. Electric modulus and interfacial polarization in composite polymeric systems. *J. Mater. Sci.* **1998**, *33*, 2027–2037.

(23) Yang, J.; Melton, M.; Sun, R.; Yang, W.; Cheng, S. Decoupling the Polymer Dynamics and the Nanoparticle Network Dynamics of Polymer Nanocomposites through Dielectric Spectroscopy and Rheology. *Macromolecules* **2020**, *53*, 302–311.

(24) Carroll, B.; Cheng, S.; Sokolov, A. P. Analyzing the Interfacial Layer Properties in Polymer Nanocomposites by Broadband Dielectric Spectroscopy. *Macromolecules* **2017**, *50*, 6149–6163.

(25) Gotro, J.; Yandrasits, M. Simultaneous dielectric and dynamic mechanical analysis of thermosetting polymers. *Polym. Eng. Sci.* **1989**, *29*, 278–284.

(26) Shepard, D. D.; Twombly, B. Simultaneous dynamic mechanical analysis and dielectric analysis of polymers. *Thermochim. Acta* **1996**, *272*, 125–129.